Population and rotational kinetics of the rhodamine B monomer and dimer: Picosecond transient spectrometry

Arthur L. Smirl, James B. Clark, E. W. Van Stryland, and B. R. Russell

Center for Applied Quantum Electronics, Department of Physics, North Texas State University, Denton, Texas 76203
(Received 16 February 1982; accepted 30 March 1982)

We use picosecond excite-and-probe techniques at 532 nm, a subnanosecond fluorescence spectrometer, and a transient-transmission spectrometer with picosecond temporal resolution to measure the population kinetics and rotational diffusion of aqueous rhodamine B monomer and dimer. The excited-state lifetimes of the monomer and dimer are determined to be 1.6 ns and 100 ps, respectively, and the rotational randomization time of the monomer is measured to be 250 ps. The dimer rotational diffusion time is determined to be longer than that of the monomer, indicating that there is a large molecular species in equilibrium with the monomer.

I. INTRODUCTION

One of the most recent and significant applications of large organic dyes of the xanthene family has been that of the active media for lasers. The widespread use and application of dye lasers has caused considerable attention to be focused on the spectroscopic characterization of these commonly used dyes. Early spectroscopic investigations of rhodamine B[1-5] indicated that the absorption spectra and fluorescence quantum yield of this dye varied greatly with a change in solvent or solute concentration. In fact, although there is considerable disagreement concerning the structure of the aqueous rhodamine B dimer, there is general agreement that these organic molecules tend to aggregate and to form dimers in solution.[3,5-8] Previous experimental studies[1-8] have measured the absorption, excitation, fluorescence, and phosphorescence spectra of both the monomeric and dimeric forms of this common dye. The primary decay mechanism for the excited state dimer appears to be nonradiative in nature; however, to our knowledge, there has been no measurement of this rapid, nonradiative excited-state dimer decay. Here we report the use of various picosecond spectroscopic techniques to measure the population kinetics and rotational diffusion of the aqueous rhodamine B monomer and dimer. Specifically, in Sec. II, we describe the use of picosecond excite-and-probe techniques at 532 nm to measure the dynamic anisotropic absorption saturation of various concentrations of aqueous rhodamine B. This concentration dependent study allows the extraction of the overall anisotropic decay rate (i.e., the sum of the level decay rate and the rotational diffusion rate) for the monomer and the overall decay rate for the dimer. In Sec. III, we report a similar but separate set of concentration-dependent studies that are insensitive to the rotational kinetics of the monomer and dimer. The latter measurements allow the extraction of the excited state lifetimes of both monomer and dimer. Simultaneous consideration of the results of these two sets of experiments (Secs. II and III) allows the determination of the rotational randomization time of the monomer and allows a lower limit to be determined for the rotational diffusion time for the dimer. In a third, separate set of experiments (Sec. IV), using the identical samples, the monomer lifetime is verified by time resolving the fluorescence using a picosecond streak camera system. Finally, in Sec. V, we describe the use of a transient transmission spectrometer with picosecond temporal resolution to measure the time-resolved rotational free absorption saturation spectra of the same solutions. The results of the latter studies not only confirm the previously measured lifetimes, but provide evidence for the presence of two molecular species (monomer and dimer) that possess drastically different absorption profiles and excited state lifetimes.

II. DYNAMIC ANISOTROPIC ABSORPTION SATURATION

The laser source for all data presented here was a passively mode-locked Nd:YAG system operating at 1.06 μm. A single pulse was extracted from the mode-locked train and amplified to produce a single pulse of measured Gaussian spatial profile and Gaussian temporal distribution. This single pulse at 1.06 μm was then frequency doubled to produce a 25 ps (FWHM) optical pulse at 0.53 μm. Optical filters were inserted to remove any residual 1.06 μm radiation. For the first two experiments (Fig. 1) the picosecond pulse at 0.53 μm was divided into two parts (excite and probe) and one part was delayed with respect to the other by a controlled amount. The probe pulse was adjusted in all cases to be approximately 5% of the excitation pulse. Note that a wavelength of 0.53 μm lies near the isosbestic point in the absorbance spectra of the rhodamine B dye. The samples studied were various concentrations of rhodamine B in H_2O. Laser grade rhodamine B was obtained from Eastman Kodak and was used without further purification. The H_2O was distilled prior to use as the solvent. All studies were conducted at room temperature.

In the first experiment, the probe pulse polarization was rotated 45° with respect to the excite pulse as shown in Fig. 1(a). Both the excitation and probe were focused onto the same 1 mm (FWHM) spot in a cell containing various concentrations of rhodamine B in aqueous solution. The intensity of the excitation pulse (6 MW/cm^2) was sufficient to slightly saturate the absorption of those molecules partially aligned parallel to the pump. The pump and the probe were then separated spatially

 0021-9606/82/140621-10$02.10

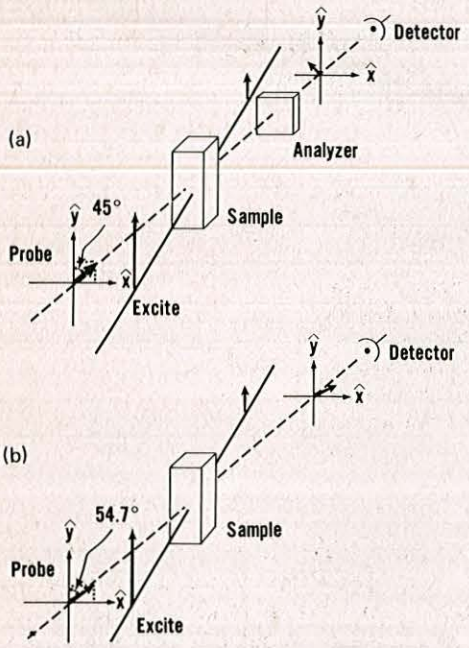

FIG. 1. Experimental configuration for the measurement of (a) the anisotropic absorption saturation and (b) the rotation-free dynamics of aqueous solutions of rhodamine B.

after they traversed the sample, and the transmission of the probe was measured through crossed polarizers, as shown. This experimental technique is identical to that used by Shank and Ippen[9] to measure the single component decay of DODCI.

Using the experimental configuration of Fig. 1(a), the probe transmission was measured as a function of time delay between excitation and probe pulses for five concentrations of aqueous rhodamine B: 4.6×10^{-3}, 9.2×10^{-4}, 4.6×10^{-4}, 9.2×10^{-5}, and 4.6×10^{-5} M. The data for these concentrations are presented in Fig. 2. The data for the 9.2×10^{-4} M solutions are omitted from the figure for clarity.

Following anisotropic saturation of the sample by the excitation pulse, the parallel polarization component of the probe experiences a larger transmission than the perpendicular component. The net result is a rotation of the probe polarization. The time-resolved measurement of the rotation of the polarization of the probe provides a convenient separation of the decay of the anisotropic saturation from the isotropic saturation. Assuming a two component solution of dimers and monomers, modeled as simple three level systems, the instantaneous transmission T_{cp} through the crossed polarizers of Fig. 1(a) is given in the small saturation limit by

$$T_{cp}(t)=C[\eta(t)+(\sigma_d/\sigma_m)^2(D/M)\beta(t)]^2\,, \tag{1}$$

where C is a concentration-dependent constant, σ_d is the dimer absorption cross section, σ_m the monomer absorption cross section, D the number of dimers, and M the number of monomers and where $\eta(t)$ and $\beta(t)$ are time-dependent integrals defined by

$$\eta(t)=\int_{-\infty}^{t} I_e(t')\exp[-(1/\tau_m)(t-t')]dt' \tag{2}$$

and

$$\beta(t)=\int_{-\infty}^{t} I_e(t')\exp[-(1/\tau_d)(t-t')]dt'\,. \tag{3}$$

In Eqs. (2) and (3), $I_e(t)$ denotes the temporal excitation intensity profile, and $1/\tau_m$ and $1/\tau_d$ are the overall monomer and dimer decay rates, respectively. Each overall decay rate is the sum of a level decay rate and a rotational diffusion rate

$$1/\tau_m=1/\tau_{1m}+1/\tau_{om} \tag{4}$$

and

$$1/\tau_d=1/\tau_{1d}+1/\tau_{od}\,, \tag{5}$$

where τ_{1m} and τ_{om} are the monomer excited-state lifetime and orientational randomization time, respectively, and τ_{1d} and τ_{od} are the dimer excited-state lifetime and orientational randomization time. Clearly, the above equations have been written to include the finite width of the excite in determining the instantaneous analyzer transmission. If this pulse width is negligible, $\eta(t)$ and $\beta(t)$ become simple exponentials. The effect of the finite width of the probe pulse on the transmitted probe energy $S(\tau)$ is determined by convoluting the instantaneous analyzer transmission $T_{cp}(t)$ with the probe temporal intensity profile $I_p(t)$ to obtain

$$S(\tau)=\int_{-\infty}^{\infty} T_{cp}(t)I_p(t-\tau)dt\,, \tag{6}$$

where τ is the probe delay. Note that all effects of the coherent coupling between pump and probe near zero delay have been neglected in the above development. It is clear from the above equations (even if the probe and excitation pulse widths are negligible) that the decay of the probe transmission (induced dichroism) is a complicated function of four parameters: the excited-state level decay of the monomer and the dimer and the orientational diffusion of the monomer and the dimer.

Extraction of measured decay constants by fitting experimental data to the above equations requires that the ratio of the number of dimers to number of monomers D/M for each concentration be determined and that the

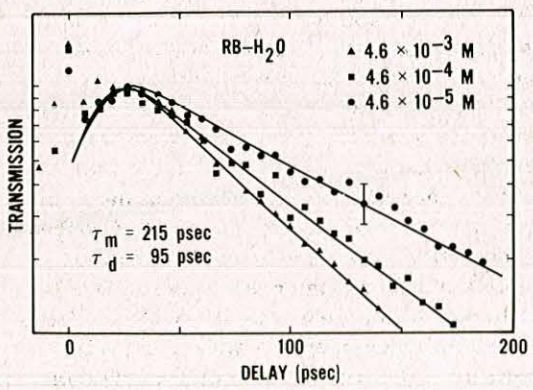

FIG. 2. The probe pulse transmission, in arbitrary units, as a function of time delay between excitation and probe pulses for the geometry of Fig. 1(a) and for three concentrations of rhodamine B in H_2O, 4.6×10^{-3}, 4.6×10^{-4}, and 4.6×10^{-5} M. The solid lines are numerical fits to the data, as discussed in the text. Two intermediate concentrations are not shown for clarity.

Table I. EQUILIBRIUM DATA FOR THE CONCENTRATION-DEPENDENT DIMERIZATION OF AQUEOUS RHODAMINE B.

Concentration, c(M)	Mole-Fraction of Monomer, X	Dimer/Monomer Ratio: D/M = $\frac{(1-x)}{2x}$
4.6×10^{-3}	0.24	1.61
9.2×10^{-4}	0.45	0.61
4.6×10^{-4}	0.57	0.38
9.2×10^{-5}	0.82	0.11
4.6×10^{-5}	0.89	0.06

ratio of the dimer and monomer absorption cross sections σ_d/σ_m be known. Fortunately, the monomer–dimer equilibrium of aqueous rhodamine B can be described by the simple mass-action expression

$$K = 2x^2 c/(1-x) , \tag{7}$$

where K is the equilibrium constant, x is the mole fraction of monomer and c is the concentration. The mole fraction of monomer x and the dimer-to-monomer number ratio D/M were determined for concentrations between 4.6×10^{-3} and 4.6×10^{-5} M using an equilibrium constant[5] of 6.8×10^{-4}M/l. These results are tabulated in Table I. In addition, a dimer-to-monomer cross section ratio σ_d/σ_m of 2.4 at 0.532 μm was extracted from the spectroscopic data of Selwyn and Steinfeld.[5]

The solid lines in Fig. 2 represent numerical fits of Eqs. (1)–(6) to the experimental data using the constants supplied in Table I. The best visual fits to the data for all five concentrations (only three shown) were obtained for an overall monomer decay time $\tau_m = 215$ ps and an overall dimer decay time $\tau_d = 95$ ps. The deviation of theory from experiment near zero delay is a result of neglecting coherent coupling effects.

It is important to remember that the overall decay constants depend on both rotational diffusion and excited-state decay [see Eqs. (4) and (5)]. Thus, an overall dimer decay constant of 95 ps suggests that the dimer is either undergoing a rapid excited state decay or an orientational relaxation at twice the rate of the monomer. Given that the dimer is expected to have the larger molecular volume, the latter would seem unlikely. Consequently, it is desirable to perform room-temperature experiments that allow the measurement of the excited state lifetimes of the monomer and dimer under the same experimental conditions as those used in this induced dichroism experiment.

III. ROTATION-FREE DYNAMICS

To facilitate the separation of the various rotational diffusion and excited-state decay times, a second separate set of concentration-dependent measurements was performed using a geometry in which the probe transmission was insensitive to rotational kinetics.[10] The experimental configuration, as shown in Fig. 1(b), was similar to that used in the first experiment, but differed in two important respects. The probe polarization was rotated to 54.7° with respect to the excitation polarization, and the analyzer polarizer was removed. Again the same five concentrations of aqueous rhodamine B were investigated using this technique to determine separately the monomer and dimer level decay. The data for three of the concentrations are shown in Fig. 3.

The change in the instantaneous sample transmission (i.e., the difference between the transient transmission and the linear, Beer's Law transmission) for the geometry of Fig. 1(b) and for a two-component system *in the small saturation limit* is given by

$$T(t) = C'[\eta'(t) + (D/M)(\sigma_d/\sigma_m)^2\beta'(t)] , \tag{8}$$

where C' is a concentration-dependent constant and where $\eta'(t)$ and $\beta'(t)$ are time-dependent integrals given by

$$\eta'(t) = \int_{-\infty}^{t} I_e(t') \exp[-(1/\tau_{1m})(t-t')]dt' \tag{9}$$

and

$$\beta'(t) = \int_{-\infty}^{t} I_e(t') \exp[-(1/\tau_{1d})(t-t')]dt' . \tag{10}$$

Notice that when the excitation pulse width is negligible, $\eta'(t)$ and $\beta'(t)$ become simple exponentials that depend only on the level decay of the monomer and dimer, respectively, and $T(t)$ becomes a weighted, linear combination of these two simple exponentials. In the small saturation limit, then, this technique is insensitive to rotational effects. Again, the effect of the finite width of the probe pulse in determining the change in the transmitted probe energy $S(\tau)$ is calculated by convoluting the instantaneous change in sample transmission $T(t)$ with the probe temporal intensity profile $I_p(t)$ to obtain

$$S(\tau) = \int_{-\infty}^{\infty} T(t) I_p(t-\tau)dt . \tag{11}$$

The lines in Fig. 3 are numerical fits of Eqs. (8)–(11) to the data. Excited-state decay constants of $\tau_{1m} = 1.6$ ns and $\tau_{1d} = 100$ ps were extracted for the monomer and dimer, respectively.

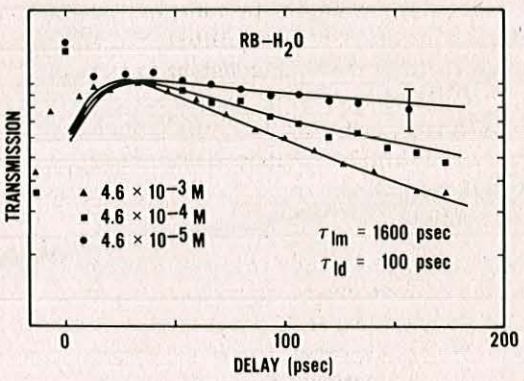

FIG. 3. The probe pulse transmission, in arbitrary units, as a function of time delay between excitation and probe pulses for the geometry of Fig. 1(b) and for three concentrations of rhodamine B in H_2O, 4.6×10^{-3}, 4.6×10^{-4}, and 4.6×10^{-5} M. The solid lines are numerical fits to the data, as discussed in the text. Two intermediate concentrations are not shown for clarity.

The overall decay constants τ_d and τ_m from the first experiment and the excited-state lifetimes τ_{1m} and τ_{1d} measured in the second were then used to determine the orientational randomization time for the monomer and dimer. Substituting $\tau_m = 215$ ps and $\tau_{1m} = 1.6$ ns into Eq. (4), we obtain a diffusion time of $\tau_{om} = 250$ ps for the monomer. Since the measured overall decay constant $\tau_d = 95$ ps and the measured excited-state lifetime $\tau_{1d} = 100$ ps are identical within experimental error, an accurate dimer rotational diffusion constant cannot be determined from Eq. (5). It is easy to show, however, that the dimer orientational randomization time τ_{od} (and therefore the molecular volume) must be larger than that of the monomer ($\tau_{od} \geq 400$ ps).

The excited-state monomer decay constant measured in these experiments is in excellent agreement with the 1.5 ns lifetime reported by Koester and Dowden[11] and Nakashima *et al.*[12] The room temperature excited-state dimer lifetime has not been previously reported. Although the primary decay route for the dimer is unknown, the lack of observed fluorescence at room temperature[12] suggests that this rapid decay may proceed by nonradiative channels. We comment that all excite-and-probe experiments were performed at varying levels of saturation (15%–50% of Beer's Law) for each solution to ensure that we were operating in the small saturation limit consistent with Eqs. (1)–(11). No measurable change in the decay rates was observed over this range of saturation levels.

An initial, abbreviated report of the above experiments has been published previously in letter form.[13] Serious questions remain, however, concerning the validity of the simple analysis outlined above. The experiments and discussion to follow are designed to verify (justify) the use of this model and the extraction of these lifetimes.

Clearly, the analysis outlined in this and the previous section presupposed that the rate for establishing monomer–dimer equilibrium must be slow compared to the relaxation processes under investigation. This is a reasonable assumption here, since the time constant for this equilibration process is believed to be on the order of microseconds.[6] Clearly, this model also supposes that either the excited-state equilibration rate is the same as $M \rightleftarrows D$ or that the time constant for establishing this new equilibrium is long compared to the time scales considered here. That is, the mole fraction of monomers and dimers remains unchanged upon excitation. This assumption will be discussed further in the following section.

A further supposition is that the rotational diffusion of the monomer and dimer can be described as a simple exponential. We do not separately measure the rotational diffusion. We do, however, measure the combined excited-state and rotational decay of the two-component system when the system is predominantly monomer (4.6×10^{-5} M solution of Fig. 2) and predominantly dimer (4.6×10^{-3} M solution of Fig. 2). These decays closely approximate an exponential over the appropriate time range and are, consequently, consistent with Eqs. (1)–(6). Note, however, that, as predicted by Eqs. (1)–(6), the decays are never perfectly exponential. Moreover, we measure the excited-state lifetime, independent of rotational effects, when the system is predominantly monomer (4.6×10^{-5} M solution of Fig. 3) and when it is dimer (4.6×10^{-3} M solution of Fig. 3). Again, these results are consistent with the analysis of this section.

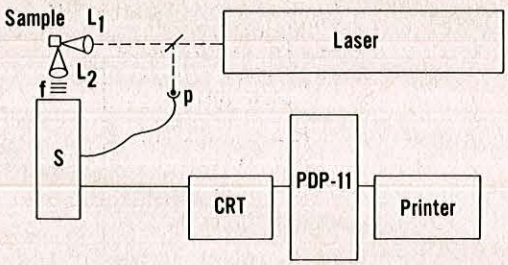

FIG. 4. Experimental arrangement for subnanosecond time-resolved fluorescence measurements.

IV. TIME-RESOLVED FLUORESCENCE

Recent reports[12,14] suggest that energy transfer from the excited state monomers (M^*) to ground state dimers (D) might play an important role in the overall excited state decay processes of moderate to concentrated solutions of rhodamine B. The analysis used to extract the excited-state dimer lifetime assumed no interaction between monomers and dimers on a subnanosecond time scale. If a significant number of excited-state monomers were deactivated through energy transfer to ground-state dimers, the population of excited monomers would be expected to decay more rapidly at higher concentrations (i.e., the monomer lifetime would not be constant). This transfer process would then generate excited state dimers in addition to those produced through saturation. Consequently, it is necessary to determine the contribution of energy transfer in aqueous systems of RB in the concentration range of 4.6×10^{-3}–4.6×10^{-5} M. This was accomplished by performing time-resolved fluorescence measurements on all five of the concentrations used in the experiments of Secs. II and III. Since the dimer has not been observed to fluoresce at room temperature, we assume that any observed fluorescence can be attributed to the monomer and that any fast fluorescent decay can be attributed to energy transfer from the monomer to the nonradiatively decaying dimer. These measurements were performed with the fluorescence apparatus shown schematically in Fig. 4.

The excitation source for these experiments was a frequency-doubled, mode-locked Nd:YAG laser identical to the laser described in the previous sections. Attempts were made to limit the energy in the green (532 nm) picosecond pulses to 0.05 mJ or less. The excitation pulse was then focused with a 100 mm focal length lens (L_1) to a spot on the surface of the sample cell (5 mm×10 mm fluorescence cuvette). The diameter of the spot was approximately 1 mm (FWHM). Sample fluorescence was collected with an identical 100 mm focal length lens (L_2), was passed through several filters

to remove scattered green excitation radiation, and was then imaged on the input slits of a Hamamatsu C979/1000/1098 streak camera system (S). This system is basically an ultra-high-speed (10 ps temporal resolution) time-resolved photometer. The streak camera was triggered by a fast photodiode, and the signal recorded by the camera was transferred to a CRT video terminal for viewing. Fluorescence traces were then transferred to a PDP-11 laboratory computer for storage or processing.

No change in the fluorescence decay rate was observed over the concentration range 1×10^{-3}–5×10^{-5} M. For example, a fluorescence trace of a 9.2×10^{-4} M solution is shown in Fig. 5. The solid line through the data is a single exponential with a decay constant ($1/e$) of 1.50 ns. This is in excellent agreement with the previously reported values[11,12] for the monomer fluorescence lifetime and with the value extracted from the excite-probe measurements of a dilute solution (4.6×10^{-5} M) in the previous sections. However, for the most concentrated solutions, a more rapid fluorescent decay was observed. For example, the fluorescence decay was noticeably faster for a concentration of 4.6×10^{-3} M than for 9.2×10^{-4} M. An excited-state fluorescence decay curve for the former solution is shown in Fig. 6. Again, the solid line through the data is a single exponential with a decay constant ($1/e$) of 820 ps.

In order to determine how this concentration dependence of the monomer lifetime affects the analysis used in Secs. II and III, suppose that the following simplistic rate equations describe the excited-state populations of the monomers and dimers following excitation:

$$\frac{dM^*}{dt} = -\tau_{lm}^{-1} M^* - \tau_T^{-1} M^* \tag{12}$$

and

$$\frac{dD^*}{dt} = -\tau_{ld}^{-1} D^* + \tau_T^{-1} M^* \,, \tag{13}$$

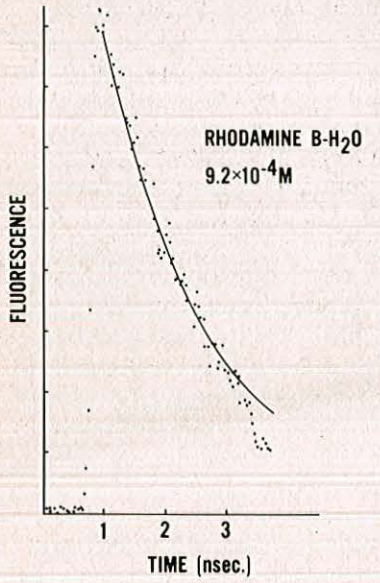

FIG. 5. Temporally resolved fluorescence of a 9.2×10^{-4} M aqueous solution of rhodamine B.

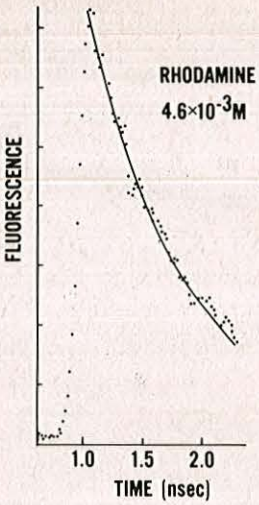

FIG. 6. Temporally resolved fluorescence of a 4.6×10^{-3} M aqueous solution of rhodamine B.

where M^* is the concentration of excited-state monomers and D^* is the concentration of excited-state dimers. That is, we assume that the excited-state monomers and dimers experience a single exponential decay with time constants τ_{lm} and τ_{ld}, respectively, and for the moment, we only allow for energy transfer from the excited-state monomer to the ground-state dimer at a rate τ_T^{-1}. We remark that τ_T^{-1} is concentration dependent and is proportional to the ground-state dimer population. Of course, we also implicitly assume that we do not deplete the ground state of either species (i.e., small saturation limit). The solutions to Eqs. (12) and (13) are

$$M^*(t) = M_0^* \exp[-(\tau_{lm}^{-1} + \tau_T^{-1})t] \tag{14}$$

and

$$D^*(t) = D_0^* \exp(-\tau_{ld}^{-1} t) + M_0^* T^{-1}(\tau_{lm}^{-1} + \tau_T^{-1} - \tau_{ld}^{-1})^{-1} \times\{\exp[-\tau_{ld}^{-1} t] - \exp[-(\tau_{lm}^{-1} + \tau_T^{-1})t]\} \,, \tag{15}$$

where M_0^* and D_0^* are the number of initially excited monomers and dimers, respectively.

Clearly, Eqs. (14) and (15) are concentration dependent. For low concentrations, such as the 9.2×10^{-4} M solution of Fig. 5 or weaker, the energy transfer rate from excited-state monomer to ground-state dimer τ_T^{-1} will be small, since there will be few ground-state dimers present. Thus, from the fluorescent decay shown in Fig. 5, we can extract a monomer lifetime τ_{lm} of 1.5 ns. We assume that τ_{lm} is independent of concentration. The largest concentration used in the data presented in Secs. II or III is 4.6×10^{-3} M. Consequently, we can use Fig. 6 to extract an overall monomer excited-state decay $\tau_{lm}^{-1} + \tau_T^{-1}$ of 820 ps. This implies a monomer to dimer energy transfer time of $\tau_T = 1.8$ ns for (and only for) this concentration. Therefore, at the very highest concentrations, our measurements suggest that energy transfer can be a primary pathway for the decay of the excited-state *monomer*, resulting in a shortening of the overall monomer excited-state lifetime by approximately a factor of 2. Nevertheless, by

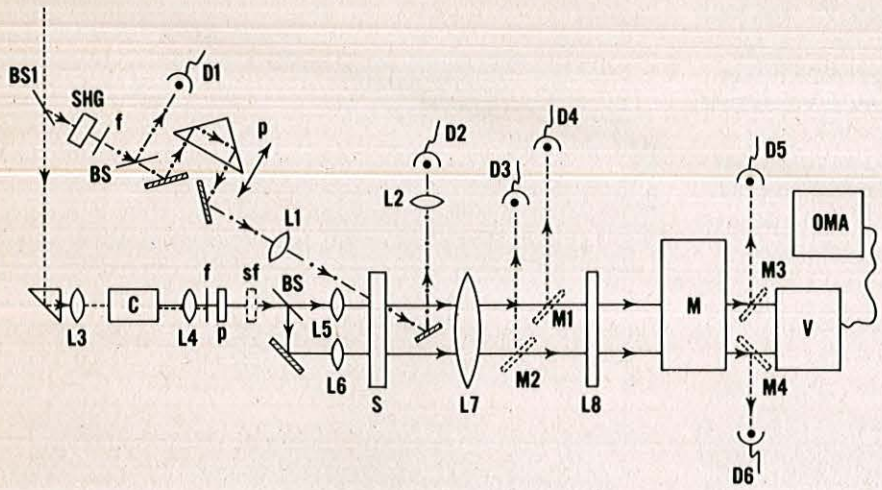

FIG. 7. Schematic of a picosecond transient transmission spectrometer that uses a picosecond white light source.

inserting the above measured values for τ_{1m} and τ_T into Eq. (15), along with the previously measured value for τ_{1d} of 100 ps, and by using Table I together with Eqs. (1) and (8), it is straightforward to show that, *at high dye concentrations*, the dimer contribution to the overall decay of the saturation dominates the measurements of Secs. II and III. Consequently, we emphasize that the techniques used in Secs. II and III for the determination of the rotational diffusion rates and excited state lifetimes of the monomer and dimer were insensitive to the apparent energy transfer processes described in this section.

V. TEMPORALLY AND SPECTRALLY RESOLVED TRANSIENT TRANSMISSION

The determination of the excited state lifetimes of the rhodamine B monomer and dimer from the anisotropic saturation measurements of Secs. II and III required that several assumptions be made. The major assumption was that, once the monomer and dimer were promoted to their respective excited electronic states, the excited molecules then returned to the ground state without any photodegradation, photoisomerization, or any interaction with one another. Again, these limiting suppositions were required in order to develop a model which would allow the extraction of the excited-state lifetimes from the single wavelength saturation experiments of a two-component system of monomers and dimers.

As an example of a possible fast dimer decay route, that we are unable to reject based on our measurements to this point and that is in violation of our assumption of independent systems of monomers and dimers, consider the following. Once the dimer has been excited to the first singlet level S_1 it again would be expected to decay rapidly to the lowest vibrational level of S_1. The exact nature of the decay of S_1 is unknown and could be a dissociation of the excited state dimer into a ground state monomer and an excited state monomer. The production of a monomer in the ground state would allow the monomer to participate in absorption processes accounting for the apparent fast ground-state recovery that we have associated with the dimer. On the other hand, if the lowest singlet state of the dimer is energetically lower that that of the monomer, as suggested by Chambers *et al.*,[8] dissociation of the dimer could result in the formation of a ground state monomer and a monomer in a high vibrational level of the ground state. Relaxation of the vibrationally excited species could occur in a few picoseconds. The overall result of this dissociation would be the formation of two ground state monomers with the observed 100 ps decay being a measure of the dimer dissociation and monomer vibrational relaxation. Since both monomer and dimer absorb at the excite-probe wavelength of 532 nm, we are not able to isolate these processes in the measurements described in Secs. II and III. Ideally, we would like to perform picosecond transient anisotropic absorption saturation experiments of the kind described in Sec. III by saturating the sample at a single wavelength (532 nm) and by probing the anisotropically bleached sample over a wide range of wavelengths. An apparatus for performing such measurements has been constructed and is described below.

A single optical pulse at 1.06 μm with a duration of 35 ps (FWHM) was extracted from the output of the model-locked Nd:YAG laser described in Sec. II. This pulse was then amplified to an energy of approximately 8 mJ. Following amplification, this intense pulse was then directed to the apparatus shown in Fig. 7. A small portion (roughly 10%) of this incident pulse was reflected by a beam splitter (BS1) to provide the excitation pulse for this experiment. The excitation pulse wavelength was then doubled to 0.532 μm by a type I lithium iodate frequency-doubling crystal (SHG), and all residual 1.06 μm radiation was removed by interference filters (f). The majority of the green excitation pulse was directed to a moveable delay prism, while a small portion of that pulse was reflected from a beam splitter (BS) into a suitably filtered detector (D_1) to serve as a reference. Following the delay prism, the excitation pulse was focused by a 333 mm focal-length lens (L_1) to a 1 mm spot within the sample. Upon exiting the sample, the transmitted excitation pulse was reflected by a mirror, recollimated by a lens (L_2), and directed to another suitably filtered PIN photodiode detector (D_2). Monitoring the ratio of the energy measured by D_2 to

that measured by D_1 yields the overall transmission of the sample. By placing filtration in the excitation path prior to the sample, we adjusted the level of saturated transmission to 1.5 times that of the Beer's Law sample transmission.

The major portion of the initially incident 1.06 μm pulse was transmitted by beam-splitter BS1 and was directed by a right angle prism to the probe-producing portion of the apparatus. The intense incident 1.06 μm pulse was focused with another 333 mm focal-length lens (L_3) into a 10 cm quartz-windowed stainless steel cell (C). The cell contained a mixture of H_2O and D_2O (1:1) that was used as the medium for generating a picosecond continuum.[15-22] The distance between lens L_3 and the continuum cell was adjusted such that the resulting beam focus lay approximately three quarters of the way through the cell. The continuum, with a peak intensity centered near 1.06 μm, extended from the infrared into the ultraviolet spectral region.[23,24] The scattered continuum was crudely recollimated by a 60 mm focal-length lens (L_4). Following collimation, the continuum was passed through several 1.06 μm rejection filters (f) to remove the remainder of the infrared pulse. The maximum efficiency for production of the continuum was approximately 75%. The continuum probe was then passed through a Glan–Taylor polarizer (P) that was adjusted to transmit optical radiation polarized at 54.7° with respect to the excite polarization, to allow the performance of rotation-free transient transmission experiments of the type analogous to those described in Sec. III. Following the polarizer, the probe is shown passing through an optical narrow band filter (sf) that selects specific probe wavelengths from the continuum. This filter is only present during the initial, or calibration, phase of the studies to be described later. The probe was then split by a beam splitter (BS) into two pulses of roughly the same energy. The portion that passed through the beam splitter was focused by a lens (L_5) into the same volume within the sample as the excitation pulse. Emerging from the sample, this pulse was recollimated by L_7 and either (a) reflected by an optical (removable) mirror M1 into a filtered detector (D4) during one of the initial calibration procedures (to be described below) or (b) focused onto the entrance slit of a monochromator (or spectrometer) by a cylindrical lens (L_8). The part of the probe pulse that was reflected by the beam splitter traveled in a parallel path to the first probe and was focused by a lens (L_6) into a region of the sample far removed from the excited region to provide a reference for determining the linear (or Beer's Law) transmission. This second probe, like the first, was then recollimated by lens L_7 and either (a) reflected by an optional (removable) mirror M2 into a filtered detector (D3) during calibration or (b) focused onto a separate point on the entrance slit of the monochromator (or spectrometer) by a cylindrical lens (L_8). The slit of the monochromator is parallel to the plane of the figure. We remark that the grating device, denoted by M, with entrance and exit slits in place could be used as a monochromator or, with exit slits removed, could be used as a spectrometer. When the grating device was used as a monochromator, the output was directed by mirror M3 to a detector D5; however, when the device was used as a spectrometer the output was imaged onto a vidicon detector and displayed by a multichannel analyzer (OMA).

To prove that the picosecond continuum was a suitable probe, two calibration experiments were performed. In the first of these, we attempted to reproduce the measurements of Sec. III. That is, we measured the sample transmission with both excitation and probe wavelengths at 0.532 μm and with the probe polarization rotated 54.7° with respect to the excitation polarization. The probe wavelength was fixed by placing a narrow band filter (sf) (5 nm bandwidth) immediately after the polarizer P as shown in Fig. 7. Mirrors M1 and M2 were also in place as shown. Thus, the experimental configuration was almost identical to that used for the rotation-free excited-state lifetime measurements of Sec. III and shown in Fig. 1(b). The primary difference was the method of generating the probe. For these experiments, the probe intensity was approximately 0.1% of the excitation. Because of the weak nature of the probe, the probe detectors were set on the highest sensitivity available, resulting in a signal-to-noise ratio of approximately 20 to 1. The use of an automated data acquisition system allowed discrimination against poorly developed continua arising from laser intensity fluctuations. By setting upper and lower limits (in the software) on acceptable probe energies, data were acquired only for laser pulses which produced continua that were similar. This resulted in rejection of the data for approximately 90% of the laser firings. Although the data taken with the filtered continuum probe were noisier (or had more scatter) than those taken with a probe produced by second harmonic generation (as in Sec. III), the two sets of data were in good agreement.

The second calibration experiment was identical to the first except that all frequency components of the picosecond continuum were allowed to traverse the sample. For this experiment, the spike filter (sf) and the mirrors M1 and M2 used in the first calibration procedure were removed. The two continua were then focused onto separate points on the input slit (slit in the plane of Fig. 7) of a 0.22 m monochromator by a cylindrical lens. The monochromator, equipped with 1.25 mm slits and a 1200 line/mm grating that was blazed at 500 nm, had a spectral band pass of 5 nm. The two probes were then spatially separated and directed to detectors D5 and D6 by removable mirrors M3 and M4. The primary advantage of this configuration over the previous one is the ability to monitor the sample transmission at any wavelength simply by setting the monochromator to that wavelength. The monochromator was set to 0.532 μm, and the rotation-free excited-state lifetime measurements of Sec. III were again repeated. Once again, the agreement between the two sets of data was good. The significance of this agreement is that all wavelength components (infrared through visible) of the probe traversed the excited region of the sample without altering the overall decay of the excited sample.

Notice that in this configuration the probe spectrum is sufficiently broad to contain the wavelength at which

the monomer fluorescence is maximum (0.590 μm). Thus, it is possible that this wavelength could be amplified by stimulated emission as it traverses the excited region. To investigate this suggestion, the monochromator was adjusted to a wavelength of 0.590 μm. Very little monomer or dimer absorption occurs at this wavelength,[5] but it is very near the fluorescence maxima of the rhodamine B monomer. The transient transmission of the probe at this wavelength is shown in Fig. 8. The large error bars (relative to those known in Secs. II or III) and noisy data are thought to be caused by the irreproducible nature of the nonlinear optical generation of the probe. Since neither the dimer nor monomer absorb at this wavelength, the initial increase in transmission following excitation is attributed to transient gain (i.e., probe amplification by the excited-state monomer population). The solid line is the convolution of probe intensity envelope (25 ps, FWHM) with an exponential 1.6 ns decay. This is the excited-state lifetime for the monomer extracted in Sec. III. It is clear then that, although this wavelength of the multiwavelength probe experiences gain (and induces excited-state depopulation), it does not affect the ground state recovery measurement, primarily because no stimulated emission can occur until the delayed probe arrives.

Summarizing, using this second calibration configuration, we monitored the transient transmission (gain) at 0.590 μm near the fluorescence peak of the monomer, and for concentrated solutions, we measured a slow decay consistent with the expected excited-state monomer lifetime. Probing at 0.532 μm, in a spectral region where both monomers and dimers participate, a fast decay was observed. These results suggest that the rapid decay can be, in fact, attributed to the presence of the dimers in concentrated solutions as was suggested in preceeding sections.

Finally, we modified the apparatus of Fig. 7 by removing the exit slit assembly of the monochromator, by removing mirrors M3 and M4, and by imaging the dispersed spectra of the two probe pulses onto a vidicon detector. Mirrors M1 and M2 and the spike filter (sf) were omitted from this configuration, as well as the previous one. The resolution of the modified spectrometer was limited to 8 nm. The rotation-free transient transmission spectra of a 9.2×10^{-4} M solution of rhodamine B in water were measured at five fixed delays

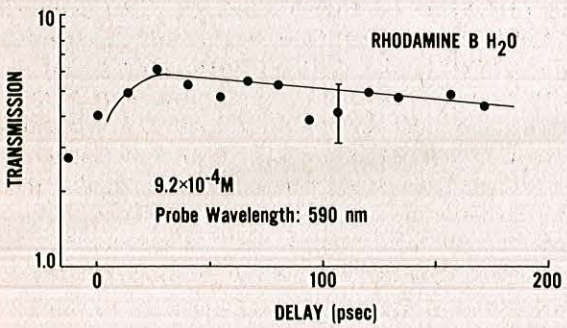

FIG. 8. Transient transmission (in arbitrary units) of 9.2×10^{-4}M solution when the probe wavelength is chosen to be 590 590 nm.

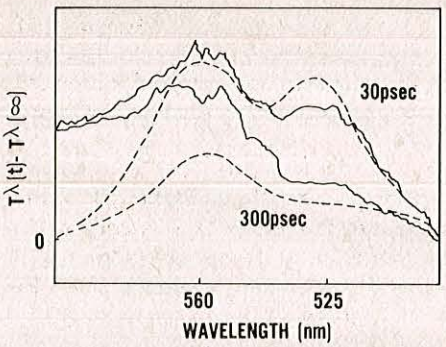

FIG. 9. A comparison of the experimental and calculated transient transmission difference spectra of a 9.2×10^{-4} M solution of aqueous rhodamine B for time delays of 30 and 300 ps.

(−50, 30, 100, 200, and 300 ps) using this apparatus. The transient transmission difference spectra for time delays of 30 and 300 ps are shown in Fig. 9. The difference spectrum is defined as $T^{\lambda}(t)-T^{\lambda}(\infty)$, where $T^{\lambda}(t)$ is the transient transmission at wavelength λ and time t, as determined by the continuum probe that traverses the excited region and where $T^{\lambda}(\infty)$ is the Beer's Law transmission at λ as determined by the continuum probe that traverses the unexcited region. The maximum transient transmission difference was observed at ~30 ps. All other delays smoothly fit the trend shown here. Although the spectra are quite noisy, a qualitative interpretation of the transient transmission is possible.

The dominant features of the transmission difference spectrum at the 30 ps delay are two maxima at approximately 560 and 523 nm. In the absorption spectrum of concentrated aqueous solutions of rhodamine B, the short wavelength maximum occurring at approximately 520 nm has been assigned as the peak absorption of the rhodamine B dimer.[5] Therefore, the maximum appearing at 523 nm in the transient transmission spectra is attributed to the saturation of that absorption. Similarly, the maximum at 560 nm in the transient transmission difference spectra is attributed to monomer saturation, as well as a small contribution from the wings of the dimer saturation. As the delay was varied from 30–300 ps, the difference peak at 523 nm was observed to disappear rapidly, consistent with a dimer lifetime of approximately 100 ps as deduced in Secs. II and III earlier. By contrast, the transmission difference at a wavelength of 560 nm decayed to only approximately 80% of its maximum value. We do not believe that even this small change was caused by monomer decay, but rather was caused by a rapid decay of the wings of the dimer saturation that overlap this spectral region. The broken lines in Fig. 9 are calculated difference spectra generated using wavelength-dependent versions of Eq. (8), the equilibrium information from Table I, the absorption profiles from Ref. 5, and the lifetimes for the monomer and dimer extracted in Sec. III. The calculated curve for the 30 ps delay was scaled to the maximum of the experimental curve. As can be seen from the figure, the experimental spectrum does not appear to decay as fast as we have predicted, but the spectral profiles are similar. The most dramatic deviation be-

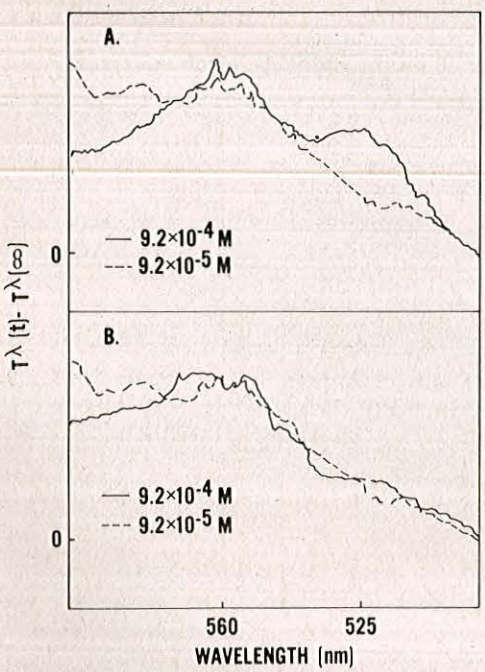

FIG. 10. A comparison of the transient transmission difference spectra (a) of dilute and concentrated solutions of rhodamine B both taken 30 ps after excitation and (b) of the dilute solution 30 ps after excitation and the concentrated solution 300 ps after excitation.

tween measurement and calculation is evident for the longest wavelengths shown. Here, the measured saturation is much larger than predicted by our simple calculation. This observation is consistent with the observation of transient gain near 590 nm, as discussed earlier in this section in connection with Fig. 8.

In order to verify that the transmission at 523 nm could be attributed to contributions from the dimers, transient-transmission measurements were performed on a weak 9.2×10^{-5} M solution of aqueous rhodamine B. The procedure used for procuring the difference spectra was identical to that used for the more concentrated solution. Although data were collected at the same optical delays (−50, 30, 100, 200, and 300 ps) as in the investigation of the concentrated solution, we show data only for the transient transmission difference spectrum for 30 ps following excitation in Fig. 10(a). Very little change was observed in the difference spectra between 30–300 ps. For comparison, the difference spectrum for a concentrated solution is normalized and plotted in Fig. 10(a) against the spectrum for the weaker solution. A cursory examination of the transient spectrum of the dilute solution reveals no maximum at 523 nm, just a monotonic rise in transmission from about 490 nm to a plateau at 560 nm. The majority of the transient signal in the region from 570–590 nm is believed to arise from transient gain of the sample, as discussed earlier. The lack of a transient dimer maximum at 523 nm is not surprising since a distinct dimer peak is also absent in the ground state absorption spectrum of the 9.2×10^{-5} M solution. Table I indicates that the dimer/monomer ratio for the dilute solution is 0.11 while this ratio is 0.61 for the 9.2×10^{-4} M solution. From this comparison, it is reasonable to assume that the rapidly decaying maximum at 523 nm is associated with the dimer molecules. Further support for this assumption is shown in Fig. 10(b), where the relaxed difference spectrum (300 ps) of the 9.2×10^{-4} M solution is compared to the maximum transient difference spectrum (30 ps) of the 9.2×10^{-5} M solution, which contains few dimers. These two spectra are virtually identical, verifying that the 523 nm maximum is associated with the aqueous rhodamine B dimer.

VI. SUMMARY

The population kinetics and the rotational diffusion of the aqueous rhodamine B monomer and dimer have been measured by using picosecond pulses from a mode-locked Nd:YAG laser to induce and time resolve the concentration-dependent transient absorption saturation of various aqueous solutions of this organic dye. Summarizing, we have used picosecond excitation and probe techniques at 0.532 μm to measure the excited-state lifetimes of the rhodamine B monomer and dimer at 1.6 ns and 100 ps, respectively, and to determine the rotational randomization time of the monomer as 250 ps. The dimer rotational diffusion time was determined to be longer than that of the monomer ($\geq$ 400 ps). The extremely short excited-state dimer lifetime of 100 ps is an indication that the dimer may decay by a rapid nonradiative process. In addition, the longer measured rotational decay time for the dimer provides physical evidence for the presence of a larger molecular species (dimer) in equilibrium with the monomer in the aqueous solution of rhodamine B. In a second experiment, using a picosecond streak camera, we time resolved the fluorescence from dilute and concentrated aqueous solutions to provide an independent measurement of the monomer excited-state lifetime and to provide evidence for energy transfer from the excited-state monomer to ground-state dimers in *very* concentrated solutions. This energy transfer was shown not to affect our determination of other decay rates.

In a final, separate set of experiments, we used a transient transmission spectrometer with picosecond temporal resolution to measure the time-resolved rotational free absorption saturation spectra of the same solutions. These observations not only confirmed the above reported lifetimes, but provided direct evidence for the presence of two molecular species that possess drastically different absorption profiles and excited state lifetimes.

ACKNOWLEDGMENTS

The authors wish to thank the members of the Center for Fast Kinetics Research at the University of Texas, Austin for allowing us to conduct the time-resolved fluorescence studies at their facility. This work was supported by The Robert A. Welch Foundation, The Research Corporation, and the North Texas State Faculty Research Fund.

[1]T. Forster and E. Konig, Z. Elektrochem. 61, 344 (1957).
[2]H. Jokobi and H. Kuhn, Z. Elektrochem. 66, 46 (1962).

[3]K. K. Rohatgi and G. S. Singhal, J. Phys. Chem. 70, 1695 (1966).
[4]K. K. Rohatgi, J. Mol. Spectrosc. 27, 545 (1968).
[5]J. E. Selwyn and J. I. Steinfeld, J. Phys. Chem. 76, 762 (1972).
[6]M. M. Wong and Z. A. Schelly, J. Phys. Chem. 78, 1891 (1974).
[7]T. Kajiwara, R. W. Chambers, and D. R. Kearns, Chem. Phys. Lett. 22, 37 (1973).
[8]R. W. Chamber, T. Kajiwara, and D. R. Kearns, J. Phys. Chem. 78, 380 (1974).
[9]C. V. Shank and E. P. Ippen, Appl. Phys. Lett. 26, 62 (1975).
[10]H. E. Lessing and A. von Jena, Chem. Phys. Lett. 42, 213 (1976).
[11]V. J. Koester and R. M. Dowben, Rev. Sci. Instrum. 49, 1186 (1978).
[12]N. Nakashima, K. Yoshihara, and F. J. Willig, Chem. Phys. 73, 3503 (1980).
[13]J. B. Clark, A. L. Smirl, E. W. Van Stryland, H. J. Mackey, and B. R. Russell, Chem. Phys. Lett. 78, 456 (1981).
[14]D. R. Lutz, K. A. Nelson, C. R. Gochanour, and M. D. Fayer, Chem. Phys. (submitted).
[15]G. E. Busch, R. P. Jones, and P. M. Rentzepis, Chem. Phys. Lett. 18, 1978 (1973).
[16]D. Madge and M. W. Windsor, Chem. Phys. Lett. 27, 31 (1974).
[17]D. Madge, M. W. Windsor, D. Holton, and M. Gouterman, Chem. Phys. Lett. 29, 183 (1979).
[18]B. I. Greene, R. M. Hochstrasser, and R. B. Weisman, J. Chem. Phys. 70, 1247 (1979).
[19]J. M. Grzybowski, S. E. Sugamori, D. F. Williams, and R. W. Yip, Chem. Phys. Lett. 65, 456 (1979).
[20]R. W. Anderson, D. E. Damschen, G. W. Schott, and L. D. Talley, J. Chem. Phys. 71, 1134 (1979).
[21]R. R. Alfano and S. Shapiro, Phys. Rev. Lett. 24, 584 (1970).
[22]R. R. Alfano and S. Shapiro, Chem. Phys. Lett. 8, 631 (1971).
[23]C. Rullier and P. Kottis, Chem. Phys. Lett. 75, 478 (1980).
[24]A. Penzkofer, A. Laubereau, and W. Kaiser, Phys. Rev. Lett. 14, 863 (1973).